Influence of the volume fraction on the electrokinetic properties of maghemite nanoparticles in suspension

Ivan T. Lucas, S. Durand-Vidal, Olivier Bernard, V. Dahirel, E. Dubois, Jean-François Dufrêche, S. Gourdin-Bertin, M. Jardat, G. Meriguet, G. Roger

Influence of the volume fraction on the electrokinetic properties of maghemite nanoparticles in suspension

I. T. Lucas[c,d,*], S. Durand-Vidal[a,b], O. Bernard[a,b], V. Dahirel[a,b], E. Dubois[a,b], J.-F. Dufrêche[e], S. Gourdin-Bertin[a,b], M. Jardat[a,b], G. Meriguet[a,b] and G. Roger[a,b,f]

[a] *Sorbonne Universités, UPMC Univ Paris 06, UMR 8234, PHENIX, F-75005, Paris, France*

[b] *CNRS, UMR 8234, PHENIX, F-75005, Paris, France*

[c] *Sorbonne Universités, UPMC Univ Paris 06, UMR 8235, LISE, F-75005, Paris - France*

[d] *CNRS, UMR 8235, LISE, F-75005, Paris, France*

[e] *Institut de Chimie Séparative de Marcoule, ICSM, UMR 5257 CEA-CNRS-Université Montpellier 2 - ENSCM, Bagnols-sur-Cèse, France*

[f] *Present address: ONERA, DMSC, F92320 Chatillon, France*

*corresponding author : ivan.lucas@upmc.fr

Influence of the volume fraction on the electrokinetic properties of maghemite nanoparticles in suspension

We used several complementary experimental and theoretical tools to characterize the charge properties of well-defined maghemite nanoparticles in solution as a function of the volume fraction. The radius of the nanoparticles is equal to 6 nm. The structural charge was measured from chemical titration and was found high enough to expect some counterions to be electrostatically attracted to the surface, decreasing the apparent charge of the nanoparticle. DC conductivity measurements were interpreted by an analytical transport theory to deduce the value of this apparent charge, denoted here by "dynamic effective charge". This dynamic effective charge is found to decrease strongly with the volume fraction. On the contrary, the "static" effective charge, defined thanks to the Bjerrum criterion and computed from Monte Carlo simulations turns out to be almost independent of the volume fraction. In the range of Debye screening length and volume fraction investigated here, double layers around nanoparticles actually interact with each other. This strong interaction between nanocolloidal maghemite particles is probably responsible for the experimental dependence of the electrokinetic properties with the volume fraction.

Keywords: word; another word; lower case except names

I. Introduction

According to the DLVO theory[1], the long-term stability of charged colloidal suspensions relies on the balance between attractive van der Waals interactions and repulsive electrostatic interactions. The magnitude of these electrostatic interactions is dictated by the charge of the colloidal particle and is strongly affected by the surrounding ionic environment, i.e. the nature and the concentration of the electrolyte. Therefore, understanding the static and dynamical properties of co-ions and counterions around the colloidal particles and their dependence with the medium of dispersion is a cornerstone to predict the long-term stability of charged colloidal suspensions.

For the vast majority of inorganic colloidal systems, the surface charge of the colloidal particle results from surface crystallographic defects (missing valencies at the surface of the particles), the state of the surface depending on the surrounding medium. In the case of oxide particles in contact with an aqueous solution, the surface charge results from proton exchange with the surface oxides and is therefore pH dependent. It can be evaluated from chemical titration of the weak acidities of the colloidal particle surface in contact with strong acidic or alkaline solutions. Depending on the authors, this charge is called the intrinsic, bare, structural, titrated or surface charge. We denote this quantity the structural charge in the following text.

Due to this structural charge, there is a local electric field at the surface of the colloidal particle. If the electrostatic interaction is much stronger than thermal energy, some counterions are strongly attracted to the surface, leading to an accumulation of counterions in the vicinity of the surface of the colloidal particle. This phenomenon is called counterion condensation[2,3]. If ions possess a strong chemical affinity to the surface, they can also bind to the surface sites. The structural charge of colloidal particle is partially compensated by these counterions, so that it bears an apparent charge, which we denote by effective charge in what follows. For a given system, the value of the effective charge depends on the method used to probe or to define it. For linear polyelectrolytes, the distinction between condensed ions and free ions has been clearly established by Manning. For colloids, defining a distance below which ions are considered as electrostatically condensed is not straightforward. Bjerrum and others have made some propositions to define the effective charge based on the radial distribution functions between ions and colloidal particles at equilibrium[2]. In the following, we refer to this charge as the "static" effective charge, as it was already proposed in the literature[4,5]. It is also possible to define the effective charge as the charge involved in the linear Poisson-Boltzmann theory, and therefore in the DLVO theory. This DLVO charge

ensures that the electric field far from the colloidal particles is equivalent to the field obtained using non-linear Poisson-Boltzmann equation.

The experimental determination of the effective charge is a non-trivial problem, which is still under debates in the community. Various techniques have been used to extract an effective charge. Osmotic pressure measurements yield an estimation of the number of free ions, and therefore are linked to the effective charge as defined by Bjerrum[6,7]. Other techniques enable to characterize the structure of the suspensions, such as X-rays or neutron scattering[8,9].This structure depends on the long-range interactions between colloidal particles, and therefore on the DLVO effective charge. Finally, electrokinetic techniques, such as electrophoresis[9-12], measure an electrokinetic charge, which we call a “dynamic” effective charge in what follows, as already proposed in the literature[4,5]. As techniques and related theoretical treatments are different, the obtained results are seldom consistent.

Moreover, some standard results of the electrokinetic theories might not be adapted to the description of colloids of nanometric size. In particular, it is usually assumed that the main contribution to the electrical conductivity of the suspension is due to small ions both in the bulk and in the double layer[10]. Conversely, in classical descriptions of electrolyte solutions[13-16] every charge species contribute to the charge transport. For nanoparticles with a radius only 10 to 30 times that of small ions, the ratio between the mobilities at infinite dilution is between 1/30 and 1/10, so that neglecting the contribution of nanoparticles is questionable.

In the present work, we focus on colloidal particles of nanometric size. More precisely, we combine experimental results, analytical theory and numerical simulations to gain more insight into the concepts of static and dynamic effective charges. Other authors have addressed this issue by using numerical simulations: Lobaskin and coworkers used a combination of Lattice Boltzmann simulations and Langevin dynamics to compute effective

charges for a model system[4]. They define the dynamic charge as the structural charge decreased by the number of counterions moving with almost the same velocity as the nanoparticle in the presence of the external field. They show that, for nanoparticles of radius equal to 3 nm in a dilute and salt-free solution, strong differences appear between the static and dynamic effective charges. In particular, both charges depend differently on the structural charge of the nanoparticle: While the static charge does almost not vary for increasing values of the structural charge larger than 40, the dynamic charge does not seem to saturate even with strong values of the structural charge (Z = 120).

The dependence of the different effective charges on the volume fraction of colloids is another issue that has been scarcely addressed[5,17]. From the theoretical perspective, it is quite difficult to include the effect of volume fraction beyond the cell model description[10], for which the volume fraction dictates the size of the cells. Nevertheless, in the case where the Debye length is of the order of the size of the colloidal particles, double layers may strongly interact when the volume fraction increases, modifying the electrokinetic properties as compared to the infinite dilution.

The correlations between colloidal particles can be estimated either by using simulation methods, or other theoretical frameworks. We propose in this work to apply an analytical transport theory, which takes into account explicitly electrostatic and excluded volume interactions between every charged species. It previously enabled the accurate interpretation of the direct-current (DC) electrical conductivity of electrolytes or solutions of macroions like micellar species, as a function of their volume fraction. This approach is applied to a home-made and already widely studied system constituted of iron oxide nanoparticles (maghemite) dispersed in aqueous medium [18-20]. The maghemite particles have a mean radius of 6 nanometers. Because of their interesting magnetic properties[18,21-23], such dispersions, known as ferrofluids, are used in an increasing number of applications that strongly rely on

their colloidal stability. In this work, we first determined the structural charge of the maghemite particles using chemical titration. Then, we performed dynamic measurements to estimate the dynamic effective charge. These latter were conducted at controlled volume fractions of maghemite nanoparticles and controlled pH. We measured the DC electrical conductivity and deduced the effective charge of nanoparticles by using an analytical transport theory, called the MSA (Mean Spherical Approximation)-transport theory. This analytical theory, which takes into account explicitly interactions between every species, proved indeed to be able to predict not only the electrical conductivity of simple electrolyte solutions[14,24], but also that of micellar systems[25,26]. The electrokinetic potential of maghemite nanoparticles, which is related to the dynamic effective charge, was also measured as a function of the volume fraction from the acoustophoresis technique. Third, the static effective charge was derived from Monte-Carlo (MC) simulations using the structural charge of the maghemite particle deduced from chemical titration as input parameter. The model used accounts for electrostatic and excluded volume interactions and neglects specific chemical binding of ions to the surface. This simulation method is particularly adapted to the determination of equilibrium properties of charged systems[27], in particular for high volume fractions[28].

After a brief recall of the experimental protocols (synthesis of the colloidal suspension, preparation of the samples and electrokinetic measurements) and of the theoretical approaches (MSA-transport theory and MC simulations) in the section II, the results obtained from the different approaches are reported and discussed in section III. As we proceed to show, a dependence of the dynamic effective charge with the volume fraction clearly appears, whereas the static effective charge as computed from MC simulations turns out to be almost independent of the volume fraction.

II. Methods

II.1. Experiments

Synthesis of maghemite colloidal suspensions: Maghemite (γ-Fe_2O_3) nanoparticles were synthesized by co-precipitation of iron(II) chloride and iron(III) chloride in alkaline medium followed by acidification with nitric acid and oxidation by iron (III) (ferric nitrate) at 100 ºC [18,29-31]. The resulting colloidal suspension strongly absorbs in the visible spectrum, appearing red and dark even at low volume fractions. The particle size determined from AFM measurements[19] follows a log-normal distribution, with a median diameter d_0=12 nm (ln d_0=<ln d>) and a polydispersity of σ=0.28. The volume fraction f of the maghemite particles was evaluated from a chemical titration of iron[31] and from atomic absorption spectroscopy.

Determination of the particle's structural charge: Maghemite nanoparticles through the pH-dependent protonation/deprotonation of their surface oxide groups turn either positively charged, uncharged at the point of zero charge (PZC) or negatively charged, according to the equilibria (1) and (2) where M is the metal of the spinel nanoparticles, $M\text{-}OH_2^+$ the metal-oxide acid site and $M\text{-}O^-$ the metal-oxide basic site.

$$\textbf{(1)}\ \mathbf{M\text{-}OH_2^+ = M\text{-}OH + H^+} \quad \text{and} \quad \textbf{(2)}\ \mathbf{M\text{-}OH = M\text{-}O^- + H^+}$$

The number of charged groups on the surface as a function of pH can be determined from titrations. This has been done here using the method already applied in [19]: the initial stable suspension at pH around 1.5 is neutralized by addition of a base up to pH = 7, which is the point of zero charge of maghemite[32-35], where flocculation is complete. The supernatant is removed and the particles are washed with distilled water until the conductivity reaches the one of water. This final state, where the particles are uncharged and the solvent is free of ions, is the starting point of the titrations performed by addition of nitric acid. Note that the particles can be perfectly redispersed in water as soon as their charge is high enough, typically

for pH < 3.5. The charge is given by the difference between the number of added H^+ and the number of H^+ determined from the pH measurements. Two totally independent experiments are plotted in Figure 1 down to pH=2.3, showing a maximal difference of 10%. Note that, below pH = 2, the accuracy of the determination of the structural charge is poor and should be considered with care since the amount of free H^+ becomes large compared to the amount of H^+ on the surface of the particles. At pH=3.1 considered here, the determination is reliable and the structural charge equals Z_b = 392. As the radius of the colloid is close to 6 nm, Z_b corresponds to a significant surface charge density of 0.87 e nm^{-2} (0.14 $C.m^{-2}$), consistent with other determinations in similar systems of iron oxides[36].

Preparation of samples of controlled volume fraction and pH: The acidic colloidal maghemite suspension (pH range 1.5-1.8) was packed into a dialysis tubing permeable to water molecules and ions (Spectrapore-12000-14000) and immersed into an acidic solution (HNO_3, pH 2.7) containing 5% in weight of Dextran polymer (500 kg mol^{-1} Amersham Biosciences). Even after several days, an asymmetric distribution of protons from both sides of the dialysis tube membrane (pH=3.1 inside vs pH=2.7 outside) is still observed and accounts for the presence of charged nanoparticles inside the tube because of the Donnan effect[37,38]. Successive dilutions of the resulting colloidal suspension at constant pH 3.1 with a nitric acid solution provided a series of samples with volume fractions f between 5.8 % and 0.0001 %.

DC conductivity measurements: The conductivity of the series of samples prepared in nitric acid HNO_3 at pH = 3.1 was measured without any other additional salt. Conductivity measurements were conducted on each sample by using a Fuoss-Kraus conductivity cell immersed into a water bath with controlled temperature (T = 25±0.1°C). The cell constant, 0.1785 cm^{-1}, was determined using the method of Lind, Zwolenik, and Fuoss[39] with high purity (99.99 %) KCl aqueous solutions. The impedance of the solution was measured with a high accuracy Wayne-Kerr bridge (model 6425 A) at four frequencies (1, 2, 5 and 10 kHz),

and the real part was extrapolated to infinite frequency to separate the contribution of the electrode polarisation and determine the resistance of the solution[40].

Electrokinetic potentials measurements: The electrokinetic potential of maghemite nanoparticles or zeta-potential in the same series of samples was measured by using the acoustophoresis technique. This technique detects the electrical potential or current generated when a suspension containing charged species is exposed to an ultrasonic wave. These quantities depend both on the density and on the charge of the solutes. We used a DT 1200 (Dispersion Technologies, USA) electro-acoustic spectrometer. This instrument measures the induced current (amplitude and phase) named CVI (Colloidal Vibration Intensity) when an ultrasonic wave is applied, and extracts the dynamic mobility of the colloidal particles. Calibration of the instrument with a suspension of Ludox® (silica particles, TM-50 Sigma Aldrich, w = 10 % in KCl at 0.01mol L^{-1} and pH=9, ζ = -38 mV) is required. The electrokinetic potential is deduced from the measured CVI using the extended Helmholtz-Smoluchowski equation[11] and several input data for maghemite particles and solvent, i.e. volume fraction, density, sound speed and dielectric constant. Unfortunately, no access to the raw data is possible from this device, so that the validity of the approximations involved in the treatment of the measures cannot be checked.

II.2. Theoretical approaches

MSA-transport theory: The DC electrical conductivity of a solution is a non-trivial function of the diffusion coefficients of ions at infinite dilution, of the charge of ions, of their concentration and of the interactions between charged species. The MSA-transport theory[24-26] provides an analytical expression of the conductivity, taking into account the deviations from the ideal behavior, namely the interactions between solutes. In the framework of this transport theory, which describes the solvent as a continuous medium characterized by its dielectric constant and its viscosity, two corrective terms are calculated[41]. The first one

accounts for the electrostatic relaxation of the ionic atmosphere around charged species after an external force is applied on the solution (due to the electric field here). The second one accounts for the hydrodynamic couplings mediated by the solvent that tend to equalize the ion drift velocities (electrophoretic phenomena). This electrophoretic effect is generally greater than the first one. The explicit formulation of those corrections is given elsewhere[25,26]. Another interest of the MSA-transport theory is that it allows one to compute the contribution of each species *i* to the global conductivity.

Several parameters are needed to compute the relaxation and electrophoretic corrections: the self-diffusion coefficient at infinite dilution of charged solutes (denoted by D°), their charge, and the minimal distance of approach between solutes, which can be reduced to an individual radius for each species (denoted by R). For small ions (H^+, NO_3^-), these parameters were taken from the literature[42]: $D°(NO_3^-) = 1.902\ 10^{-9}\ m^2s^{-1}$, $D°(H^+) = 9.310\ 10^{-9}\ m^2s^{-1}$ (deduced from the individual electrical conductivity at infinite dilution of H^+), $R(NO_3^-) = 0.19$ nm, $R(H^+) = 0.095$ nm (which corresponds to the size of a water molecule) [13]. We checked that these parameters allowed us to predict the conductivity of dilute HNO_3 solutions with a good precision. The diffusion coefficient at infinite dilution of maghemite particles is calculated thanks to the Stokes-Einstein relation from the radius of the particle (6 nm): $D°(\text{maghemite}) = k_BT / (6\pi\eta R)$ with k_B the Botzmann constant, T the temperature and η the viscosity of water at ambient temperature. The only unknown parameter is thus the charge of maghemite nanoparticles, taken as an adjustable parameter to model the experimental conductivity. This charge accounts for interactions at long range between moving nanoparticles and is thus an effective dynamic charge, denoted by $Z_{eff,dyn}$ in what follows, i.e. the effective charge of the nanoparticle moving with some of its counterions under the influence of the external electric field.

Monte Carlo simulations: Monte Carlo numerical simulations allow one to compute the average thermodynamical properties of a model system included in a simulation box of length L_{box} with periodic boundary conditions. Here, we were particularly interested in the radial distribution functions between charged solutes in the suspension, with the solvent treated as a continuum. The MC technique is particularly adapted to the simulation of solutions of charged nanoparticles in the presence of small ions[43-46]. If one focuses on the pair distribution function $g_{Cj}(r)$ between nanoparticles and ions of type *j*, the number N_{Cj} of ions *j* situated at a distance *r* from the center of a nanoparticle can be easily determined using equation (5):

$$N_{Cj}(r) = \int_0^r n_j 4\pi r_1^2 g_{Cj}(r_1) dr_1 \quad (5)$$

where n_j is the bulk concentration of ions *j* ($n_j = N_j / L_{box}^3$ with N_j the number of ions *j* in the simulation box). From this quantity, the static effective charge $Z_{eff\text{-}static}$ of the nanoparticle can be deduced at a given distance from the nanoparticle (see below).

The electrostatic potential at a given distance *r* from a nanoparticle, which is related to the electrokinetic potential, was also computed from these simulations, by solving Poisson's equation within the spherical geometry around the nanoparticle[47]:

$$y_C(r) = \frac{1}{e} \int_r^{Lbox/2} \frac{dr_1}{r_1^2} \left[\int_{R_C}^{r_1} r_e(r_2) r_2^2 dr_2 + z_b e \right] \quad (6)$$

where $\varepsilon = \varepsilon_0 \varepsilon_r$ is the permittivity of the medium, R_C the radius of the nanoparticle, r_e the electrical density of charge around the nanoparticle, and *e* the elementary charge. In this formula, the electrical density of charge is deduced from the radial distribution functions and includes also other nanoparticles.

Monte Carlo (MC) calculations were carried out at a constant temperature of 25°C to simulate four different volume fractions of nanoparticles surrounded by their co-ions and counterions:

f = 0.1, 0.5, 1.5 and 5%. Solute particles are modeled as charged hard spheres (primitive model) because long-ranged electrostatic interactions between solutes are assumed to dominate over other interactions. The radius of nanoparticles is equal to 6 nm, and that of small ions (nitrate ions and protons) is taken equal to 0.25 nm, as it is usually done to describe simple electrolyte solutions[44]. The proton concentration corresponds to pH=3.1 as established in the experimental protocol. Each nanoparticle has a constant structural charge Z_b=392, as found from titration results. The simulation box contains 2 or 3 nanoparticles. One million steps per particle were achieved to ensure the convergence of the radial distribution functions $g_{Cj}(r)$ [44]. The parameters of the simulations are given in Table 1.

f (%)	L_{box} (nm)	$N_{nanoparticles}$	N_{NO3-}	N_{H+}
0.1	121.86	2	1649	865
0.5	81.577	3	1436	260
1.5	56.562	3	1263	87
5	37.865	3	1202	26

Table 1: Parameters of Monte Carlo simulations. f (%) volume fraction of nanoparticles, L_{box} the length of the cubic simulation box, N_i the number of particles i in the simulation box.

III. Results

The DC electrical conductivity of the maghemite suspension as a function of the volume fraction of nanoparticles at constant pH (pH=3.1) is presented on Figure 2 (black squares). We have used the MSA-transport theory to deduce from these experimental results the dynamic effective charge $Z_{eff\text{-}dyn}$ of maghemite nanoparticles (fitting procedure explained in Section II.2). It was not possible to account for the experiments while keeping a constant value of $Z_{eff\text{-}dyn}$ as a function of the volume fraction. We have thus repeated the fitting procedure for each volume fraction, so that we obtained the dynamic effective charge as a

function of the volume fraction. These theoretical results are also plotted on Figure 2. Moreover, the contributions of each charged species to the global conductivity were computed and are plotted as a function of the volume fraction in maghemite on Figure 3. The electrokinetic potential of maghemite nanoparticles in the same samples, measured by acoustophoresis for volume fractions larger than 0.5 %, is plotted on Figure 4.

This first set of results calls for several comments. First, at this specific pH, the contribution to the electrical conductivity of protons is of the order of 0.03 $S.m^{-1}$, as it can be easily evaluated from the individual electrical conductivity at infinite dilution. Their contribution to conductivity is constant with volume fraction. As shown by the MSA-transport calculations presented in Figure 3, the contributions of maghemite nanoparticles and nitrate ions prevail over that of protons for volume fractions higher than 2 %. Second, the effective charge of nanoparticles as deduced from MSA-transport calculations is much smaller than the structural charge, and is found to decrease with the volume fraction: $Z_{eff\text{-}dyn}$ varies between 288 at f=0.4%, and 116 at f=5.6%, whereas we found for the structural charge Z_b=392 from chemical titrations. As already stated, the effective dynamic charge as deduced from MSA-calculations accounts for the number of counterions which are sufficiently attracted by a nanoparticle to move with it under the application of an external electric field, decreasing the mobility of the nanoparticle and thus the electrical conductivity of the system. These results are corroborated by the values of the electrokinetic potential, which is found to decrease by a factor two between 0.05 % and 5.8 % (acoustophoresis measurements). The electrokinetic potential, which is the potential difference between the stationary layer of fluid attached to the nanoparticle and the value at long distance, i.e. far from any nanoparticle, depends also on the number of ions situated in the vicinity of the nanoparticle and moving with it. It appears then both from the conductivity and the electrokinetic potential measurements that the number of counterions dynamically coupled to the nanoparticle increases with the volume fraction.

Monte Carlo simulations allow us to probe the number of counterions statically coupled to the nanoparticle according to the Bjerrum criterion. Figure 5 displays the number of counterions at a given distance from the center of a nanoparticle for several volume fractions computed by simulation. We recall that in the model used in simulations, the nanoparticle bears a charge equal to the structural charge of the maghemite particles, and that solute species are treated as charged hard spheres. At a given distance *r*, one can define an effective charge equal to the structural charge minus the number of counterions N_{Cj}. Several criteria can be used for the determination of the threshold distance where counterions are no longer in strong interaction with the particle [2,44]. This optimal threshold distance is often chosen as the point where the first derivative of $N_{Cj}(r)$ is minimum (inflexion point). In the plots displayed in Fig. 5, this corresponds to distances equal to 10.4, 13.4, 15.0 and 16.1 nm from the center of the nanoparticle for volume fractions of $f = 5.0$, 1.5, 0.5 and 0.1% respectively. At these distances from the center of the nanoparticle the effective charge is found almost constant for the four systems, equal to $Z_{eff\text{-}static} = 50$. Note that this value is consistent with that defined by Belloni in a colloidal suspension[2], $Z_{eff\text{-}static} = 4\, r_{eff} / L_B$ with L_B the Bjerrum length (we have $Z_{eff\text{-}static} = 58$ for $r_{eff} = 10.4$ nm). Nevertheless, these results differ from those obtained previously for the dynamic effective charge in two aspects: i) the value of the static effective charge is much lower than those of the dynamic effective charge, ii) the effective charge is found almost independent of the volume fraction.

The fact that the effective static charge is found to be lower than the dynamic effective charge can be relatively easily understood. Some of the counterions, assumed to be strongly electrostatically coupled to the nanoparticle according to the Bjerrum criterion, actually are not sufficiently "bound" to move with the nanoparticle in the presence of an external field, so that the dynamic effective charge estimated by the MSA-transport theory is larger than the static one. This result was already obtained by Lobaskin et al.[4] from theoretical

investigations. The variation of the dynamic effective charge and of the electrokinetic potential with the volume fraction of nanoparticles is not easy to interpret. In standard electrokinetic theories (Helmholtz-Smoluchowki limit) where the Debye layer is very thin, electrokinetic properties of colloids are usually assumed to be independent on the volume fraction. In our case, particles are of nanometric size and in solution with low concentration of added salt (NO_3^- and H^+ ions in the diluting HNO_3 solution of pH 3.1). To evaluate the Debye length, we can assume either that only the ions of the nitric acid in the bulk participate to the electrostatic screening, or, more realistically, that both counterions of the nanoparticles and ions of the nitric acid in the bulk participate to the screening. In the first case, we find a Debye length κ^{-1} equal to 10.7 nm, whereas in the second case, κ^{-1} varies between 1.6 nm (at ϕ=5%) and 6.3 nm (at ϕ=0.1 %). This means that in every case, and whatever the choice to evaluate the Debye length, we have κR close to one, with R the radius of the maghemite nanoparticle. In other words, we cannot neglect the size of the double layer compared to that of the nanoparticle. Monte Carlo simulation results bring more insights into this issue. We have plotted in Fig. 6 the electrostatic potential created by a nanoparticle and charged species as a function of the distance to the center of the nanoparticle. The electric potential presents in every case a minimum, because several nanoparticles are included in the simulation box. We have translated the computed values so that the minimum of the electric potential corresponds to zero. For the highest volume fraction investigated here, double layers around nanoparticles interact with each other, as attested by the fact that the computed electric potential does not provide any plateau in between nanoparticles. The electric potential is then strongly influenced by the presence of other nanoparticles. This strong interaction between nanocolloidal maghemite particles is probably responsible for the experimental dependence of the electrokinetic phenomena with the volume fraction.

IV. Discussion and Conclusion

In this study we exposed several complementary experimental and theoretical tools to characterize the ionic condensation on well-defined maghemite nanoparticles in solution. More precisely, the combination of DC conductivity measurements, acoustophoresis, analytical theory, and numerical simulations allows us to investigate the influence of the volume fraction of nanoparticles on their charge, a key parameter which helps understanding the stability of the suspensions.

Our results show the following trends for such nanocolloidal systems:

(1) The effective charge deduced from dynamic measurements, called here the dynamic effective charge or the electrokinetic charge, is different from the static effective charge deduced from the structure of the ionic cloud at equilibrium. It is indeed found much larger than the static effective charge, which indicates that most of the electrostatically condensed ions (from Bjerrum's definition of condensation) are not fixed relative to the nanoparticle surface and therefore contribute to the electrical current. This means that in the present case, the precise definition of the position of the slip plane where the electrokinetic potential is defined is not straigthforward[11].

(2) The dynamic effective charge appears to decrease while the volume fraction of the maghemite nanoparticles increases. This result, determined from conductivity measurements treated within the Mean Spherical Approximation-transport theory, is also confirmed by electroacoustic measurements. It is not usual to observe such a dependence of the properties of the colloidal particles on the volume fraction. This might occur in our systems because it stands at the limits of the colloidal domain. The small size of the colloidal particle together with its important surface charge have indeed several consequences: (i) the concentration of counterions becomes very important even for low nanoparticles volume fractions, and is therefore often larger than the concentration of the added salt, (ii) the average distance between individual particles is much smaller than in the case of micrometer colloidal particles

for the same volume fraction, so that at a given Debye screening length, increasing the volume fraction leads to strong interactions between the double layers of neighboring nanoparticles, and (iii) charged nanoparticles participate to the charge current within the solution, and therefore influence the displacements of other nanoparticles. As a consequence, the properties of the solution should be influenced by the volume fraction of colloids. For all these reasons, our choice to resort to a model of the solution that explicitly considers the effect of all charged species (salt ions, charged nanoparticles and their counterions) was necessary.

(3) The static effective charge does not vary with the volume fraction, which shows again that the electrokinetic charges and the static effective charge are not straightforwardly related quantities.

It is generally accepted that the distribution of ions around colloidal particles cannot be simply described by a succession of layers with clear-cut boundaries and well-defined properties[48]. Our results suggest that, for the present system, condensed counterions fall into the following two categories: electrostatically condensed counterions which move with the nanoparticles and do not contribute to the electrical current (those leading to $Z_{eff\text{-}dyn}$), and the electrostatically condensed ions which participate to the electrical conduction (those leading to $Z_{eff\text{-}stat}$). While the total number of condensed counterions per particle almost does not vary with the volume fraction of nanoparticles, the populations of each category of ions does.

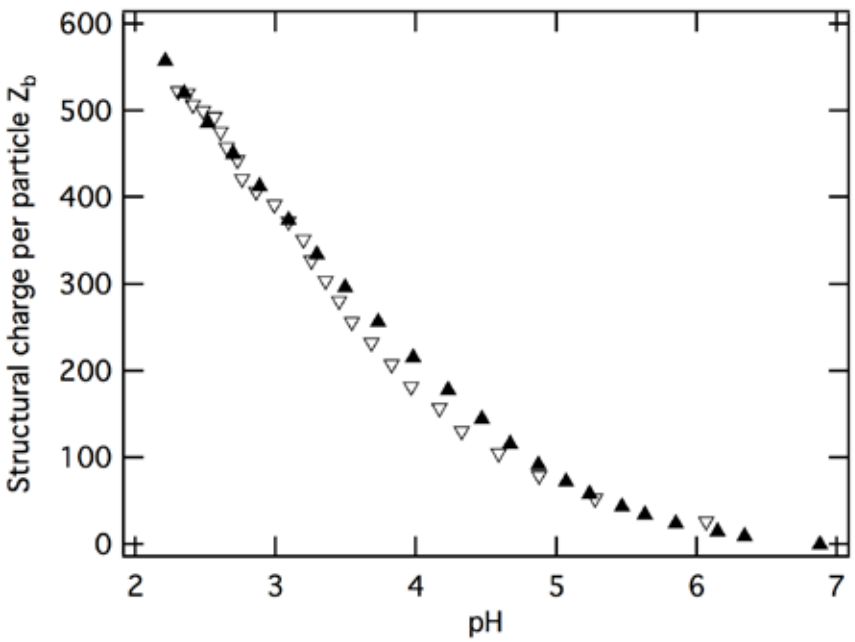

Figure 1: Structural charge Z_b of maghemite nanoparticles determined from chemical titration at a nanoparticle volume fraction of Φ =1.5% (see text for details).

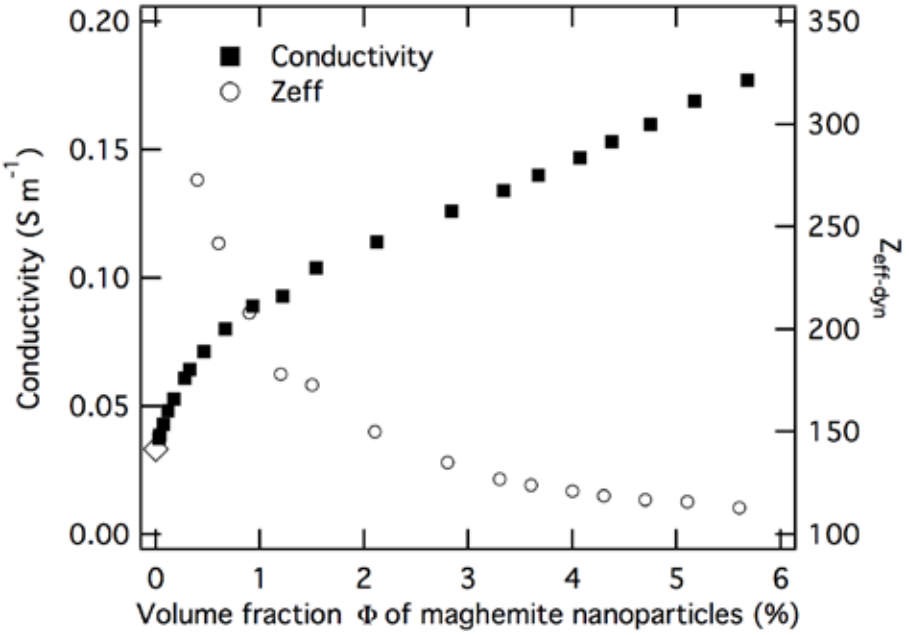

Figure 2: Experimental electrical conductivity of samples of maghemite nanoparticles prepared in HNO_3 at pH=3.1, as a function of the volume fraction of nanoparticles (left scale, squares). Electrical conductivity of pure HNO_3 at zero volume fraction (diamond shape). Dynamic effective charge of maghemite nanoparticles as determined from a fitting procedure

by using the MSA-transport theory to account for the experimental conductivity (right scale, circles).

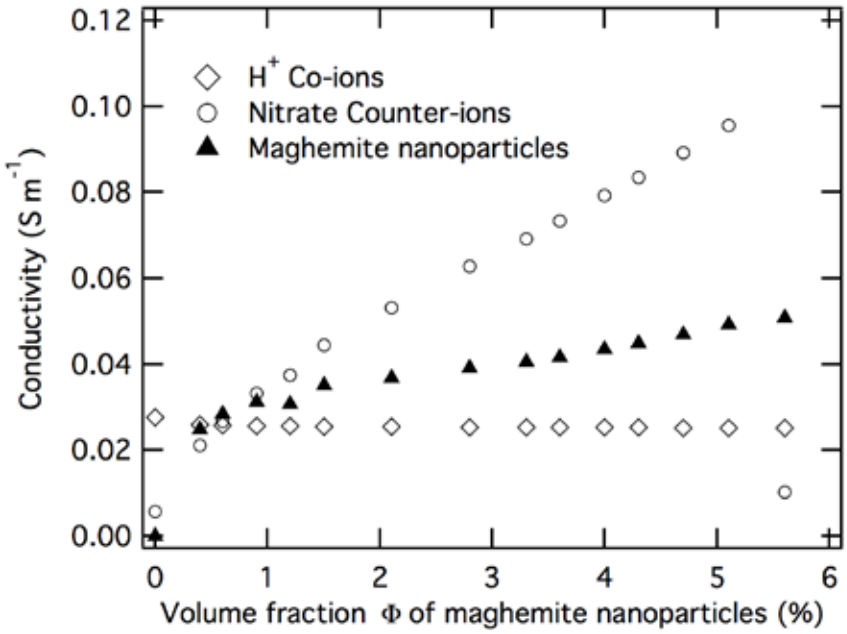

Figure 3: Contribution to the electrical conductivity of the different charged species as a function of the volume fraction **f** of maghemite nanoparticles as computed by the MSA-transport theory. Nanoparticles surrounded by adsorbed counterions, bearing a dynamic effective charge (full triangles), free NO_3^- counterions (empty circles) and H^+ co-ions (empty diamonds).

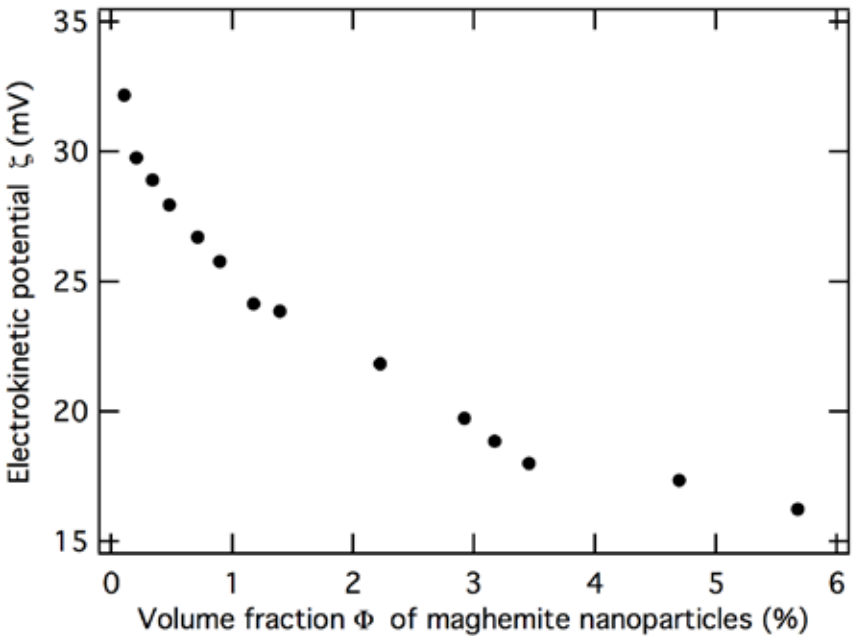

Figure 4: Electrokinetic potential or zeta-potential (***z)*** of maghemite nanoparticles prepared in HNO_3 at pH=3.1 determined by acoustophoresis as a function of the volume fraction *f* of nanoparticles.

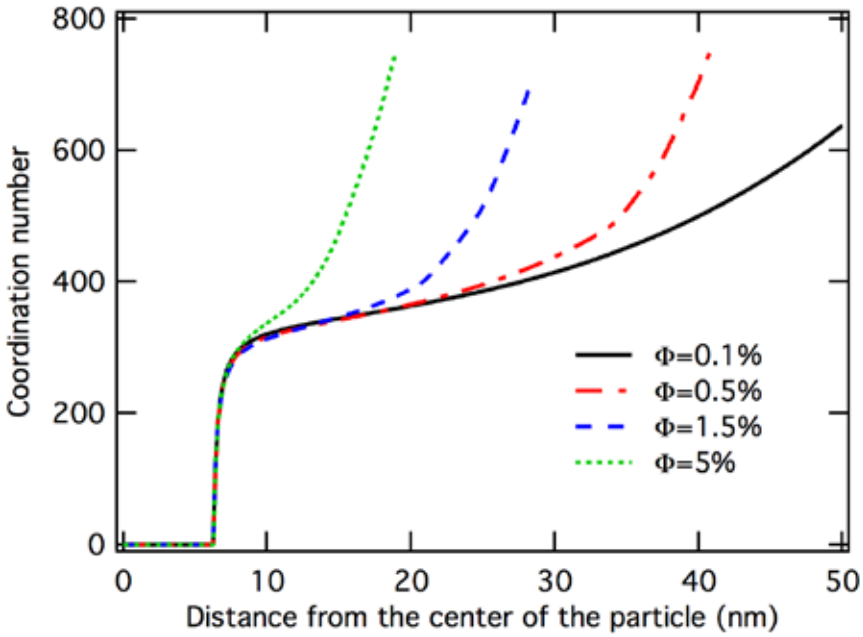

Figure 5: Number of NO_3^- counterions as a function of the distance to the center of maghemite nanoparticles deduced from the radial distribution functions computed from Monte Carlo simulations for four different volume fractions. Plots end in each case at $L_{box}/2$.

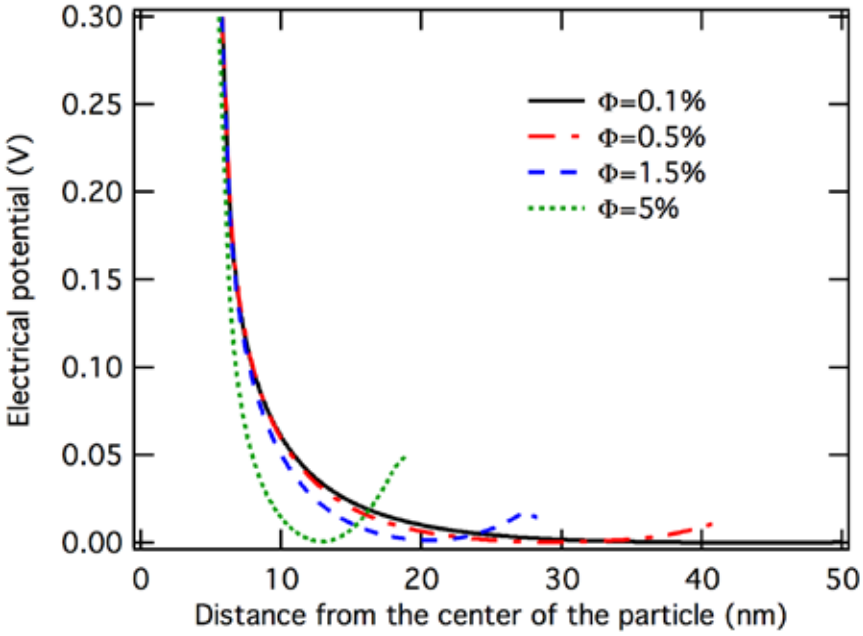

Figure 6: Electrical potential created by the nanoparticle and small ions as a function of the distance to the center of the particle deduced from the pair distribution functions computed from Monte Carlo simulations. For each volume fraction, the values were rescaled so that the minimum of the function is set to zero.

[1]E.J.W. Verwey and J.T.G. Overbeek, *Theory of the Stability of Lyophobic Colloids: The Interactions of Sol Particles Having an Electric Double Layer* (Elsevier, Amsterdam, 1948).
[2]L. Belloni, *Coll. Surf. a-Physicochemical and Engineering Aspects* **140** (1-3), 227 (1998).
[3]G.S. Manning, *Quart. Rev. Biophys.* **11** (02), 179 (1978).
[4]V. Lobaskin, B. Dünweg, and C. Holm, *J. Phys. Cond. Mat.* **16** (38), S4063 (2004).
[5]P. Wette, H. J. Schope, and T. Palberg, *J. Chem. Phys.* **116** (24), 10981 (2002).
[6]I. Pochard, J. P. Boisvert, A. Malgat, and C. Daneault, *Coll. Polym. Sci.* **279** (9), 850 (2001).
[7]I. Pochard, J.-P. Boisvert, J. Persello, and A. Foissy, *Polym. Int.* **52** (4), 619 (2003).
[8]D. E. Kuehner, J. Engmann, F. Fergg, M. Wernick, H. W. Blanch, and J. M. Prausnitz, *J. Phys. Chem. B* **103** (8), 1368 (1999).
[9]J. Lyklema, *Solid-Liquid Interfaces, Fundamentals of Interface and Colloid Science*, Vol II (Academic Press, San Diego, 1995).
[10]J.H. Masliyah and S. Bhattacharjee, *Electrokinetic and colloid transport phenomena* (Wiley Interscience, 2006).
[11]A. V. Delgado, F. Gonzalez-Caballero, R. J. Hunter, L. K. Koopal, and J. Lyklema, *J. Coll. Int. Sci.* **309** (2), 194 (2007).
[12]C. Chassagne and M. Ibanez, *Pure App. Chem.* **85** (1), 41 (2013).
[13]R. A. Robinson and R. H. Stokes, *Electrolyte Solutions* (Butterworth, London, 1959).
[14]O. Bernard, W. Kunz, P. Turq, and L. Blum, *J. Phys. Chem.* **96** (9), 3833 (1992).
[15]T. Olynyk, M. Jardat, D. Krulic, and P. Turq, *J. Phys. Chem. B* **105** (31), 7394 (2001).
[16]M. Jardat, S. Durand-Vidal, N. Da Mota, and P. Turq, *J. Chem. Phys.* **120** (13), 6268 (2004).
[17]L. Bocquet, E. Trizac, and M. Aubouy, *J. Chem. Phys.* **117** (17), 8138 (2002).
[18]B. Berkovski, *Magnetic Fluids and Applications Handbook* (Begell House, New York, 1996).
[19]I. T. Lucas, S. Durand-Vidal, E. Dubois, J. Chevalet, and P. Turq, *J. Phys. Chem. C* **111** (50), 18568 (2007).
[20]B. Frka-Petesic, E. Dubois, V. Dupuis, F. Cousin, and R. Perzynski, *Magnetohydrodynamics* **49** (3/4), 328 (2013).
[21]E. Blums, A. Cebers, and M.M. Maiorov, *Magnetic Fluids* (Gruyter New York, 1997).
[22]R. Rosensweig, *Ferrohydrodynamics* (Cambridge University Press, Cambridge 1985).
[23]S. Odenbach, *Ferrofluids : Magnetically Controllable Fluids and Their Applications* (Springer, Berlin, 2002).
[24]J.-F. Dufrêche, O. Bernard, S. Durand-Vidal, and P. Turq, *J. Phys. Chem. B* **109**, 9873 (2005).
[25]S. Durand-Vidal, M. Jardat, V. Dahirel, O. Bernard, K. Perrigaud, and P. Turq, *J. Phys. Chem. B* **110** (31), 15542 (2006).
[26]M. Jardat, V. Dahirel, S. Durand-Vidal, I. T. Lucas, O. Bernard, and P. Turq, *Mol. Phys.* **104** (22-24), 3667 (2006).
[27]V. Dahirel and M. Jardat, *Current Opinion in Colloid & Interface Science* **15** (1-2), 2 (2010).
[28]V. Dahirel and J.-P. Hansen, *J. Chem. Phys.* **131** (8) (2009).
[29]R. Massart, *Ieee Transactions on Magnetics* **17** (2), 1247 (1981).
[30]R. Massart, *C. R. Acad. Sci. Paris* **291** (1), 1 (1980).
[31]R. Massart, E. Dubois, V. Cabuil, and E. Hasmonay, *J. Mag. Mag. Mat.* **149** (1-2), 1 (1995).
[32]A. F. C. Campos, F. A. Tourinho, G. J. da Silva, M. C. F. L. Lara, and J. Depeyrot, *Eur. Phys. J. E* **6** (1), 29 (2001).
[33]M. Kosmulski, *Adv. Coll. Int. Sci.* **152** (1–2), 14 (2009).
[34]R. M. Cornell and U. Schwertmann, *The Iron Oxides: Structure, Properties, Reactions, Occurences and Uses* (Wiley VCH, Weinheim, 2003).
[35]M. Kosmulski, *Chemical properties of material surfaces*, Vol 102 (Marcel Dekker Inc., New York, Basel, 2001).
[36]A. F. C. Campos, R. Aquino, F. A. Tourinho, F. L. O. Paula, and J. Depeyrot, *Eur. Phys. J. E* **36** (4), 1, 42 (2013).
[37]F. G. Donnan, *Zeitschrift Fur Elektrochemie Und Angewandte Physikalische Chemie* **17**, 572 (1911).
[38]M. Dubois, T. Zemb, L. Belloni, A. Delville, P. Levitz, and R. Setton, *J. Chem. Phys.* **96** (3), 2278 (1992).
[39]J. E. Lind, J. J. Zwolenik, and R. M. Fuoss, *J. Am. Chem. Soc.* **81** (7), 1557 (1959).
[40]T. B. Hoover, *J. Phys. Chem.* **74** (13), 2667 (1970).
[41]L. Onsager and R. M. Fuoss, *J. Phys. Chem.* **36** (7), 2689 (1932).
[42]Y. Marcus, *Ion properties* (Marcel Dekker Inc., New York 1997).
[43]J. Z. Wu, D. Bratko, H. W. Blanch, and J. M. Prausnitz, *J. Chem. Phys.* **111** (15), 7084 (1999).
[44]V. Dahirel, M. Jardat, J.-F. Dufreche, and P. Turq, *J. Chem. Phys.* **126** (11), 114108 (2007).
[45]F. Carnal and S. Stoll, *J. Phys. Chem. B* **115** (42), 12007 (2011).
[46]F. Carnal and S. Stoll, *J. Phys. Chem. A* **116** (25), 6600 (2012).

[47]G. M. Roger, G. Mériguet, O. Bernard, S. Durand-Vidal, and P. Turq, *Coll. Surf. A: Physicochemical and Engineering Aspects* **436** (0), 408 (2013).
[48]H. Zhang, A. A. Hassanali, Y. K. Shin, C. Knight, and S. J. Singer, *J. Chem. Phys.* **134** (2) (2011).